

NASA Technical Paper 1203

LOAN COPY: RETURN
AFWL TECHNICAL LIB
KIRTLAND AFB, NM

0134560



TECH LIBRARY KAFB, NM

Characterization of Wear Debris Generated in Accelerated Rolling-Element Fatigue Tests

William R. Jones, Jr., and Richard J. Parker

APRIL 1978

NASA





NASA Technical Paper 1203

Characterization of Wear Debris Generated in Accelerated Rolling-Element Fatigue Tests

William R. Jones, Jr., and Richard J. Parker
Lewis Research Center
Cleveland, Ohio



National Aeronautics
and Space Administration

**Scientific and Technical
Information Office**

1978

CHARACTERIZATION OF WEAR DEBRIS GENERATED IN ACCELERATED ROLLING-ELEMENT FATIGUE TESTS*

by William R. Jones, Jr., and Richard J. Parker

Lewis Research Center

SUMMARY

A Ferrographic analysis was used to determine the types and quantities of wear debris generated during accelerated rolling contact fatigue tests. The NASA five-ball rolling contact fatigue tester was used. Ball specimens were made of AMS 5749, a corrosion resistant, high-temperature bearing steel. The lubricant was a superrefined naphthenic mineral oil. Conditions included a maximum Hertz stress of 5.52×10^9 pascals and a shaft speed of 10 000 rpm. Four types of debris were observed - normal rubbing wear particles, fatigue microspall particles, spheres, and friction polymer deposits. For about half of the tests, the fatigue spall particle rating and the number of spherical particles reached a maximum during the last one-third of the test durations. The number of spheres observed in these accelerated fatigue tests was much less than others have reported during long duration testing under lower loads. Laminar particles, sometimes associated with rolling contact fatigue, were not observed in this study. The characterization of wear debris as a function of time was of limited use in predicting fatigue failures in these accelerated tests.

INTRODUCTION

The goals of oil analysis are to diagnose the current condition of operating machines and to be able to predict any future problems. A variety of different techniques (ref. 1) are being employed to effect these goals. These include spectrometric oil analysis (SOAP), magnetic chip detectors, vibration sensors, and particle counters. Although each of these techniques has certain advantages, most of the techniques suffer

*Presented at the Joint Lubrication Conference sponsored by the American Society of Lubrication Engineers and the American Society of Mechanical Engineers, Kansas City, Missouri, October 3-5, 1977.

from the disadvantage of not being able to distinguish among the various wear modes that can occur.

A new instrument, the Ferrograph, has been developed which magnetically precipitates wear debris from used lubricants onto a glass slide to yield a Ferrogram (refs. 2 to 4). The precipitated particles range from approximately 0.02 to a few micrometers and are arranged according to size on the slide. Individual particles may be observed with a unique bichromatic microscope, the Ferroscope, or with a conventional scanning electron microscope.

A number of investigators (refs. 5 to 10) have identified the characteristic wear particles associated with the various wear mechanisms. In particular, three particle types have been observed during rolling contact fatigue: spheres, spalls, and laminar particles (ref. 10). In fact, the occurrence of spherical particles in oil samples has been shown to be a precursor of bearing fatigue in some cases (refs. 9 to 11).

The objective of this investigation was to use the Ferrograph to determine the types and quantities of wear particles generated during accelerated rolling-contact fatigue tests. Test materials were AMS 5749 steel balls and a superrefined naphthenic mineral oil. Tests were conducted in the NASA five-ball fatigue tester at a maximum Hertz stress of 5.52×10^9 pascals (800 000 psi), a contact angle of 30° , a shaft speed of 10 000 rpm, and a temperature of 340 K (150° F).

Mr. Vernon Westcott of Foxboro/Trans-Sonics, Inc., Burlington, Massachusetts, obtained the SEM analysis from the National Engineering Laboratory of Scotland, East Kilbride, Glasgow.

EXPERIMENTAL APPARATUS AND PROCEDURE

Five-Ball Fatigue Tester

The NASA five-ball fatigue tester was used for all tests. The apparatus is described in detail in reference 12. The five-ball fatigue tester is shown in figure 1(a) and the test assembly in figure 1(b). This fatigue tester consists essentially of an upper test ball pyramided on four lower balls that are positioned by a separator and are free to rotate in an angular-contact raceway. System loading and drive are supplied through a vertical drive shaft which grips the upper-test ball. For every revolution of the drive shaft, the upper-test ball receives three stress cycles from the lower balls. The upper-test ball and raceway are analogous in operation to the inner and outer races of a bearing, respectively. The separator and lower balls function in a manner similar to the cage and the balls in a bearing.

The 1.27-centimeter- (1/2-in.-) diameter, grade 10, VIM-VAR AMS 5749 steel balls used in these tests were from a single heat of material. A typical chemical

analysis (wt %) of this material is as follows: carbon, 1.15; silicon, 0.30; manganese, 0.50; chromium, 14.5; molybdenum, 4.0; vanadium, 1.2; and the balance iron.

Lubrication is provided by a once-through, mist lubrication system. The lubricant was a superrefined naphthenic mineral oil with a viscosity of 79×10^{-6} square meter per second (79 cS) at 311 K (100° F). No attempt was made to dry or control the moisture content of the mineral oil. It was used in the as-received condition (<50 ppm dissolved water content). Since dissolved water in a lubricant accelerates rolling contact fatigue (ref. 13), it may also affect the production of wear debris. A study is underway to determine the effect of dissolved water on wear particle generation during rolling contact fatigue.

Vibration instrumentation detects a fatigue spall on either the upper or the lower ball and automatically shuts down the tester. This provision allows unmonitored operation and a consistent criterion for failure. The test assembly is blanketed with nitrogen during operation. Tests were conducted at a maximum hertz stress of 5.52×10^9 pascals (800 000 psi). This higher than normal stress accelerates the fatigue process so that data may be obtained in a reasonable length of time. One test was conducted at a lower stress level (3.4×10^9 Pa, 500 000 psi).

Fatigue Testing Procedure

Before they were assembled in the five-ball fatigue tester, all test section components were flushed and scrubbed with ethyl alcohol and wiped dry with clean cheesecloth. The test assembly was coated with lubricant to prevent wear at startup. A new set of five balls was used for each test. Each test was suspended when a fatigue failure occurred on either a lower or an upper test ball or when a preset cutoff time was reached. The speed, outer-race temperature, and oil flow were monitored and recorded at regular intervals. After each test, the outer race of the five-ball system was examined visually for damage. If any damage was discovered, the race was replaced before further testing.

Ferrograph

The Ferrograph (refs. 2 to 4) is an instrument used to magnetically precipitate wear particles from a used oil onto a specially prepared glass slide. A mixture of 3×10^{-6} cubic meter (3 ml) of used oil and 1×10^{-6} cubic meter (1 ml) of solvent is prepared. This mixture is then slowly pumped over the slide as shown in figure 2. A solvent wash and fixing cycle follows which removes residual oil and permanently attaches the particles to the slide. The resulting slide with its associated particles is called a Ferrogram.

The amount of wear debris on a Ferrogram was determined by measuring the optical density (percent area covered) of the deposit at seven positions along the slide - entry (55-56), 54, 50, 40, 30, 20, and 10 millimeters from the end of the slide. A composite Ferrogram density was determined for each slide by averaging the seven readings.

Energy Dispersive X-ray Analysis

The elemental composition of the different types of wear debris was determined using energy dispersive X-ray analysis (EDAX). In order to prevent charging in the scanning electron microscope, the Ferrogram slides were coated with either a thin layer ($\sim 2 \times 10^{-8}$ m, 200 Å) of carbon or gold.

Sample Collecting Procedure

The five-ball fatigue test assembly is mist lubricated in a once-through system by a very small quantity of lubricant (5×10^{-7} m³/hr, <0.5 ml/hr). Lubricant samples (3 to 5×10^{-6} m³, 3 to 5 ml) were collected periodically from the gravity drain tube below the tester (fig. 1(a)). Sample times varied because of the low and sometimes varying mist flow rate. Essentially all lubricant passing through the test assembly was collected.

RESULTS AND DISCUSSION

The oil samples analyzed in this study were obtained from two series of tests included in the larger fatigue test program reported in reference 13. The two test series included a total of 52 fatigue tests, 16 of which were monitored by Ferrography. Of these 16 tests, fatigue failures occurred in 7 of them after test durations of 22 to 98 hours. The remaining 9 tests were suspensions. If a fatigue failure had not occurred by a certain preset time (~ 100 hr), the test was terminated. Test times for the suspensions ranged from 100 to 118 hours. In this study, the tests resulting in failure are designated as F-1, F-2, etc., and the suspensions as S-1, S-2, etc. A typical fatigue spall is shown in figure 3(a). An enlarged area of the spall appears in figure 3(b). The massive (~ 0.1 mm in major dimension) spall fragments resulting from the failure are easily visible.

Types of Wear Debris

Four types of wear debris consistently appeared in most samples. These types

were normal rubbing (adhesive) wear particles, fatigue microspall particles, spherical particles, and friction polymer deposits. Table I contains a summary of the wear particle types observed in this study. Three of these types are evident in figure 4, which is an optical micrograph of the Ferrogram entry deposit from test F-6 (76-hr sample).

Normal Rubbing Wear Particles

Oil samples from almost any source contain some normal rubbing wear particles. This particle type normally represents a nondestructive form of wear, and most samples in this study contained at least a few such particles. These particles consist of small ($<5\text{ }\mu\text{m}$ in major dimension and $<1\text{ }\mu\text{m}$ thick) asymmetrical metallic flakes. When many of these particles are present in a sample they will appear as strings on the Ferrograms due to the magnetic field alignment. An electron micrograph of such a string of normal rubbing wear particles appears in figure 5(a). These particles were in the oil sampled at the conclusion of the 98-hour test (F-7). Energy-dispersive X-ray analysis (EDAX) of the particle labelled A in figure 5(a) is shown in figure 5(b). The analysis indicates that the particle is from the bearing steel test specimens. Figure 5(c) contains the background EDAX analysis for the Ferrogram slide.

Fatigue Microspall Particles

Fatigue microspall particles were observed on many Ferrograms. However, these particles are not to be confused with the massive spall fragments occurring at failure and shown in figure 3(b). These macroscopic (tenths of millimeters in major dimension) spall fragments were not observed in the oil samples. These fragments remained in the test chamber since the rig and lubricant flow were shut down immediately as a spall occurred.

However, prior to fatigue failure and as the major spall is developing, microspall particles are generated. Typically, these particles were 5 to 20 micrometers long and 1 to 2 micrometers thick. They appeared as flat platelets having smooth surfaces and irregular shapes. Examples appear in figure 4. Morphologically, microspall particles are quite similar to normal rubbing wear particles. The main distinction is one of size. Microspall particles are larger and thicker.

Spherical Particles

Metallic microspheres (1 to $10\text{ }\mu\text{m}$ diam) were observed in most samples. However, most of the spheres were less than 5 micrometers in diameter. An electron micrograph of a sphere appears in figure 6(a). Typical EDAX analyses for the spherical

particles appear in figures 6(b) and (c). As can be seen, the spheres were composed of either manganese and iron or iron, chromium, vanadium, molybdenum, and manganese. The latter, of course, corresponds to the composition of AMS 5749. The origin of the iron and manganese spheres is not known. However, it should be noted that Ferrograms prepared from unused oils will sometimes contain a few spheres. Therefore, sphere counts of less than 10 are probably not significant.

Friction Polymer Deposits

Most Ferrograms contained varying amounts of friction polymer deposits. Examples of this material are shown in figures 4 and 6(a). An EDAX analysis of the deposit in figure 6(a) is given in figure 6(d). After allowing for the background elements only small amounts of iron and copper are contained in the deposit. The iron is most likely from small rubbing wear particles occluded in the deposit. Unfortunately, carbon cannot be detected by EDAX. However, it is a logical assumption that the majority of the deposit must be organic in nature.

Actually, two types of the friction polymer deposit were observed. These are illustrated in figure 7. The first type is an amorphous appearing deposit that is transparent when viewed with transmitted light and appears dark in reflected white light. This type was not observable when reflected polarized light was used with a crossed analyzer. The second type appears to be crystalline in nature. When viewed with reflected white light it appears light blue and is translucent to transmitted light. Under reflected polarized light viewed with a crossed analyzer it appears white. Most crystalline materials exhibit this type of optical behavior (birefringence). The crystals are made visible under crossed polars because of the internal scattering of the light which causes it to be depolarized.

Both forms of deposit occurred on almost all Ferrograms. The deposits were distributed throughout the length of the Ferrograms, but the total amount varied. The deposits ranged from micron size to several millimeters in diameter. There was no apparent correlation between the amounts of these deposits and the amount of metallic debris or sampling time. This material was continually formed during tests with the naphthenic mineral oil lubricant. However, no friction polymer was observed on any of the Ferrograms from the lower stress (3.4×10^9 Pa, 500 000 psi) test (S-9).

The material must be insoluble or only partially soluble in the solvents used in preparing the Ferrograms. Conceivably, if a different solvent system is used in which the material is completely soluble, its presence on the Ferrograms could be avoided.

Friction polymer deposits have been observed on Ferrograms in other studies. Polyphenyl ethers (ref. 15) produced characteristic rocklike and cylindrical organo-

metallic debris in pin-on-disk experiments. Other deposits, termed polymud, were observed with MIL-L-23699 polyester oils in rubbing wear experiments (ref. 4).

Correlation of Ferrogram Results with Fatigue Failure

One useful technique for following a developing failure is to monitor the ratio of large to small wear particles in each sample. The ratio is determined by optically measuring the percent area covered at the entry position for the large particles and at the 50-millimeter position for the small particles. Bowen and Westcott (ref. 10) have advocated using two other parameters, the general wear level parameter and the wear severity index. Both are calculated from the large and small particle measurements. All three parameters will normally increase as failure approaches. However, none of the parameters were useful in this study because of the friction polymer deposits which masked the particle density readings. The optical densitometer does not differentiate between the nonmetallic friction polymer and the metallic wear particles. Composite Ferrogram densities for each test were determined and appear in tables II and III. However, since the composite densities also reflect the varying amounts of friction polymer, no correlation exists between the fatigue results and these measurements.

The progression of the fatigue process has been studied by other investigators (refs. 6 to 11). In those studies, a precursor to fatigue failure has been the appearance of metallic microspheres in the lubricant. In addition, microspall particles and laminar particles sometimes appear in the oil prior to failure.

It would then appear that fatigue failure should be easy to predict. However, a number of problems exist which can make prediction difficult. Metallic spheres can be generated by mechanisms other than fatigue, such as grinding (refs. 16 and 17), welding (ref. 10), fretting (ref. 18), cavitation erosion (ref. 19), and possibly burnishing (ref. 20). Except for size differences, spheres from different mechanisms appear morphologically similar. Also, some rolling contact fatigue studies (ref. 21) have yielded few spheres, while others have shown that millions of spheres can be generated (ref. 11).

Another problem area is that of distinguishing between large rubbing wear particles and small fatigue spall particles. Both have similar major dimensions ($\sim 5 \mu\text{m}$) and similar morphologies, and both are thin platelets with smooth surfaces.

Bearing these problems in mind, the quantities of both particle types associated with rolling contact fatigue (spheres and microspall particles) were determined for each oil sample. Laminar particles reported by others (ref. 10) were not observed in this study. The quantity of spheres in a sample was determined by simply counting the number between approximately the 50 and 55 millimeter positions on each Ferrogram. The following rating was used for the fatigue microspall particles: few (+), several

(++), many (+++), and very many (++++). Although not associated with the fatigue process, the quantity of normal rubbing wear particles was rated in an identical manner. Values for the three particle types are summarized for each sample in tables II (failures) and III (suspensions). The composite Ferrogram densities and sample times also appear in these tables. The number of spheres as a function of test duration appears in figures 8 (failures) and 9 (suspensions). Fatigue spall particle rating as a function of test duration appears in figures 10 (failures) and 11 (suspensions). As can be seen, the results were quite variable. In some instances the increase in spheres and microspall particles with test duration was dramatic (F-6, F-7, S-2, and S-3). In other cases, there was little if any increase (F-4, F-5, and S-8). In about half of the tests (failures and suspensions), one or both of the parameters reached a maximum during the last one-third of the test durations.

When this study was initiated it was felt that the suspended tests would provide the control or baseline data. It was not appreciated that because of the accelerated nature of these tests the suspensions could also be in the process of fatiguing. The types and quantities of wear debris are quite similar from both failures and suspensions. Some test balls from suspended tests were examined to see if a fatigue process was interrupted before the primary spall could occur. Upper test balls from five suspended tests were sectioned and examined optically and in a scanning electron microscope. All examined balls showed varying degrees of surface damage (i.e., minor spalls and cracks). An example of a surface crack on the upper test ball from test S-8 (100 hr) appears in figure 12. An electron micrograph of a number of minor spalls on the upper test ball from test S-4 (100 hr) is shown in figure 13. Balls from tests S-2, S-3, and S-3 showed similar types of surface damage.

Therefore, it was felt that a test run at a reduced stress level (3.4×10^9 Pa, 500 000 psi) would provide a better baseline for comparison. At this level, fatigue progression should be slow enough that little damage would be incurred by the test balls during a 100-hour test. Suspension S-9 run at the previous reduced stress did yield different results compared to the higher stress tests. Although a few spheres were observed, there were no abrupt increases. Very few microspall particles were generated, but the number of normal rubbing wear particles appeared to increase. There was also a complete absence of friction polymer deposits.

Correlation of Results with Other Investigators

Qualitatively, the results of this study correlate with the observations of others (refs. 6, 9, 10, and 11) that microspall and spherical particles are associated with rolling contact fatigue. However, the large number of spheres (>1000/Ferrogram) observed by Middleton (ref. 11) was not confirmed in this study. The maximum number

of spheres appearing on any one Ferrogram was about 50. In addition, laminar particles (20 to 50 μm in major dimension, $<1 \mu\text{m}$ thick), which have been associated with rolling contact fatigue (ref. 10), were not observed. These differences may be related to the accelerated nature of these fatigue tests.

Predictive Capability of Ferrography

The characterization of wear debris as a function of time using the Ferrograph was of limited use in predicting fatigue failures in these tests. Because of the higher than normal stresses, the time scale for failures to occur was greatly compressed. This factor, combined with the low lubricant flow rate, limited the number of samples for analysis.

SUMMARY OF RESULTS

The major results of the Ferrographic analysis of wear debris generated during accelerated rolling contact fatigue tests may be summarized as follows:

1. Four types of wear debris were observed: Normal rubbing wear particles, fatigue microspall particles, spheres, and friction polymer deposits.
2. For about half of the tests, including failures and suspensions, fatigue microspall rating and the number of spherical particles reached a maximum during the last one-third of the test durations. For the remaining tests there was little or no increase in these parameters.
3. The number of spheres observed (<50 per $3 \times 10^{-6} \text{ m}^3$ (3 ml) sample) in these accelerated tests was much less than others have reported during long duration testing under lower loads.
4. Laminar particles, sometimes associated with rolling contact fatigue, were not observed in this study.
5. Characterization of wear debris as a function of time was of limited use in predicting fatigue failures in these accelerated tests.

Lewis Research Center,
National Aeronautics and Space Administration,
Cleveland, Ohio, January 30, 1978,
505-04.

REFERENCES

1. Beerbower, A.: Spectrometry and Other Analysis Tools for Failure Prognosis. *Lubr. Eng.*, vol. 32, no. 6, June 1976, pp. 285-293.
2. Seifert, W. W.; and Westcott, V. C.: A Method for the Study of Wear Particles in Lubricating Oil. *Wear*, vol. 21, 1972, pp. 27-42.
3. Westcott, V. C.; and Seifert, W. W.: Investigation of Iron Content of Lubricating Oil Using Ferrograph and an Emission Spectrometer. *Wear*, vol. 23, 1973, pp. 239-249.
4. Scott, D.; Seifert, W. W.; and Westcott, V. C.: Ferrography - An Advanced Design Aid for the 80's. *Wear*, vol. 34, 1975, pp. 251-260.
5. Reda, A. A.; Bowen, R.; and Westcott, V. C.: Characteristics of Particles Generated at the Interface Between Sliding Steel Surfaces. *Wear*, vol. 34, 1975, pp. 261-273.
6. Scott, Douglas; Seifert, William W.; and Westcott, Vernon C.: The Particles of Wear. *Sci. Am.*, vol. 230, no. 5, May 1974, pp. 88-97.
7. Westcott, V. C.; and Middleton, J. L.: The Investigation and Interpretation of the Nature of Wear Particles. Trans-Sonics, Inc., 1974. (Available from NT15 as AD-A003553.)
8. Scott, D.; and Mills, G. H.: Debris Examination in the SEM: A Prognostic Approach to Failure Prevention. Presented at the 7th Annual Symposium on Scanning Electron Microscopy, A Workshop on Failure Analysis and SEM, (Chicago, Ill), Apr. 1974, pp. 883-888.
9. Scott, D.; and Mills, G. H.: Spherical Debris - Its Occurrence, Formation and Significance in Rolling Contact Fatigue. *Wear*, vol. 24, 1973, pp. 235-242.
10. Bowen, E. Roderic; and Westcott, Vernon C.: Wear Particle Atlas. Naval Air Engineering Center, July 1976.
11. Middleton, J. L.; Westcott, V. C.; and Wright, R. W.: The Number of Spherical Particles Emitted by Propagating Fatigue Cracks in Rolling Bearings. *Wear*, vol. 30, 1974, pp. 275-277.
12. Carter, Thomas L.; Zaretsky, Erwin V.; and Anderson, William J.: Effect of Hardness and Other Mechanical Properties on Rolling-Contact Fatigue Life of Four High-Temperature Bearing Steels. NASA TN D-270, 1960.

13. Parker, Richard J.; and Hodder, Robert S.: Effect of Double Vacuum Melting and Retained Austenite on the Rolling-Element Fatigue Life of AMS 5749 Bearing Steel. NASA TP-1060, 1977.
14. Schatzbert, P.; and Felsen, I. M.: Effects of Water and Oxygen During Rolling Contact Lubrication. *Wear*, vol. 12, 1968, pp. 331-342.
15. Jones, William R., Jr.: Ferrographic Analysis of Wear Debris from Boundary Lubrication Experiments with a Five Ring Polyphenyl Ether. *ASLE Trans.*, vol. 18, no. 3, 1975, pp. 153-162.
16. Broszeit, E.; and Hess, F. J.: Discussion to: A Scanning Electron Microscope Study of Fracture Phenomena Associated with Rolling Contact Fatigue Failure. *Wear*, vol. 17, 1971, pp. 314-315.
17. Jones, W. R., Jr.: Spherical Artifacts on Ferrograms. *Wear*, vol. 37, 1976, pp. 193-195.
18. Stowers, I. F.; and Rabinowicz, E.: Spherical Particles Formed in the Fretting of Silver. *J. Appl. Phys.*, vol. 43, no. 5, May 1972, pp. 2485-2487.
19. Doroff, Stanley W.; et al.: Spheroidal Particles Produced by Cavitation Erosion. *Nature*, vol. 247, no. 5440, 8 Feb. 1974, pp. 363-364.
20. Rabinowicz, Ernest: The Formation of Spherical Wear Particles. *Wear*, vol. 42, 1977, pp. 149-156.
21. Dalal, H.; et al.: Progression of Surface Damage in Rolling Contact Fatigue. SKF-AL74TO02, SKF Industries, Inc., 1974.

TABLE I. - SUMMARY OF TYPES OF WEAR DEBRIS OBSERVED IN FERROGRAMS

	Type of wear debris	Morphology	Size range	Comments
Metallic	Normal rubbing wear particles	Asymmetrical flakes with smooth surfaces	<5 μm in major dimension <1 μm thick	Normally appear in strings
	Fatigue spall particles	Flat platelets with smooth surfaces, irregularly shaped perimeter	5 to 20 μm in major dimension 1 to 2 μm thick	
	Spheres	Spherical particles	1 to 10 μm in diameter	Most were <5 μm in diameter
Nonmetallic	Friction polymer	Irregularly shaped patches	Variable (from a few μm to a few mm)	Two types
				Amorphous Crystalline
				Transmitted light
				Transparent Translucent
				Reflected white light
				Dark Light blue
				Reflected polarized light with crossed analyzer
				Not observed White

TABLE II. - SUMMARY OF FERROGRAM RESULTS (FAILURES)

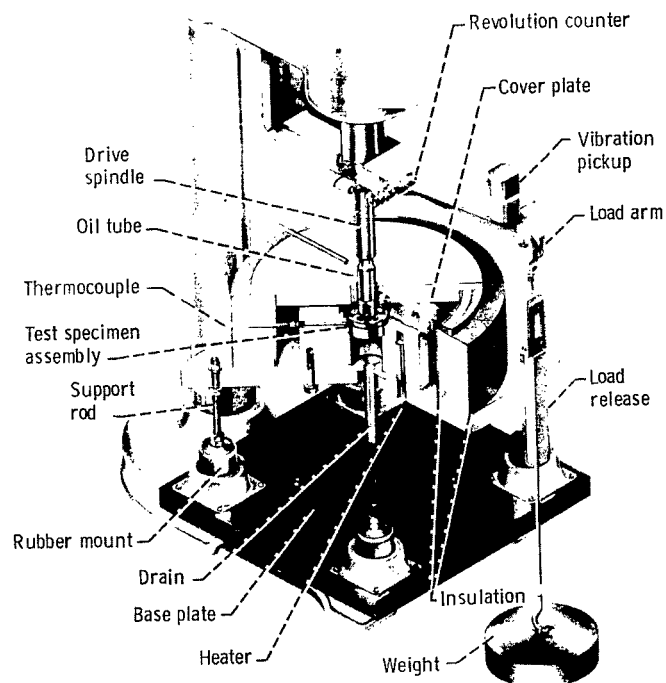
Test (failures)	Sample time, hr	Composite Ferrogram density, percent area covered	Fatigue spall particles rating ^a	Normal rubbing wear particles rating ^a	Spherical particles total
F-1	23	4.0	0	+	2
	31	9.3	0	+	2
	47	4.6	0	+	1
	49	6.5	+	++	12
	74	2.2	+	+	2
F-2	20	8.9	0	+	1
	34	10.5	0	+	2
	50	12.9	0	++	1
	58	11.1	+	++	0
	74	4.0	++	+++	3
	76	6.3	+++	++	4
F-3	22	9.2	++++	+++	8
F-4	43	8.2	0	++	0
	63	2.5	0	+	1
F-5	6	10	0	+	1
	22	3.0	+	+	1
	30	6.9	0	+	1
	47	1.7	0	+	1
	54	3.5	0	+	1
	71	3.7	0	+	1
	78	.9	+	+	3
	81	5.1	0	+	1
F-6	8	9.9	+	++	4
	36	8.9	+	+++	2
	43	11.7	0	+++	2
	67	28	+++	++++	1
	74	10.3	++	+++	7
	76	13.7	+++	++++	22
F-7	18	12	+	+	1
	25	5.9	+	+	0
	32	13	+++	+	2
	49	5.4	++++	+	6
	56	5.3	+++	+	0
	73	10.4	+++	+	1
	80	15.9	+++	+	2
	93	1.1	++++	++	16
	98	8.4	++++	+++	48

^aNone, 0; few, +; several, ++; many, +++; very many, ++++.

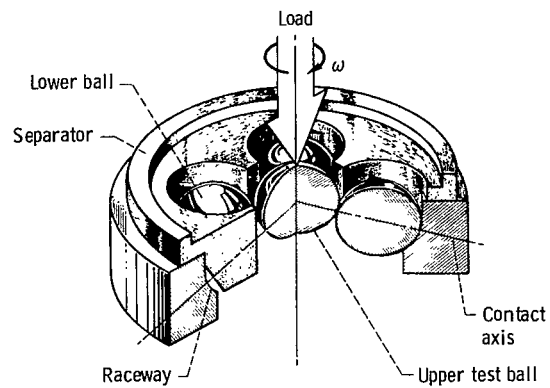
TABLE III. - SUMMARY OF FERROGRAM RESULTS (SUSPENSIONS)

Test (suspensions)	Sample time, hr	Composite Ferrogram density, percent area covered	Fatigue spall particles rating ^a	Normal rubbing wear particles rating ^a	Spherical particles total
S-1	66	3.5	0	0	0
	73	6.0	+	+	16
	89	5.5	+	+	1
	113	2.8	+	+	0
S-2	16	1.1	0	+	0
	40	^b ND	++	+	1
	54	2.7	+	+	0
	71	2.8	+	+	1
	95	ND	++	++	5
	100	ND	++	++	12
S-3	45	7.8	+	+	1
	69	1.4	+	+	0
	76	2.1	0	+	0
	100	6.9	0	+	3
	118	7.8	+++	+++	10
S-4	27	ND	0	+++	0
	49	ND	0	+	2
	57	ND	+	+	0
	73	ND	+	+	1
	81	ND	+	+	3
	103	ND	++	+	1
S-4	21	4.4	0	+	1
	46	11.4	0	+	29
	54	6.4	++	+	15
	60	5.3	+	+	5
	100	8.5	+	+	4
S-6	6	20.4	0	0	0
	29	12.6	++	+	3
	45	7.1	++	+	9
	52	10.8	9	+	0
	67	11.0	+	0	2
	113	7.7	9	+	1
S-7	64	5.2	++	+	1
	89	4.1	+++	+	4
	93	8.2	+	+	1
	101	7.8	++	+	1
S-8	42	3.6	+	+	0
	66	1.0	+	+	2
	90	2.4	0	+	0
	97	2.1	0	+	2
	100	12.7	+	+	0
^c S-9	25	3.3	+	+	5
	31	3.0	0	+++	6
	49	2.0	0	+++	1
	55	3.0	+	+++	3
	71	2.0	9	+	0
	75	1.0	0	+	1
	76	2.0	0	0	0
	100	1.0	0	+	3

^aNone, 0; few, +; several, ++; many, +++.^bNot determined, ND.^cLow stress, 3.4×10^9 Pa (500 000 psi).



(a) Cutaway view of five-ball fatigue tester.



(b) Five-ball test assembly.

Figure 1. - Test apparatus.

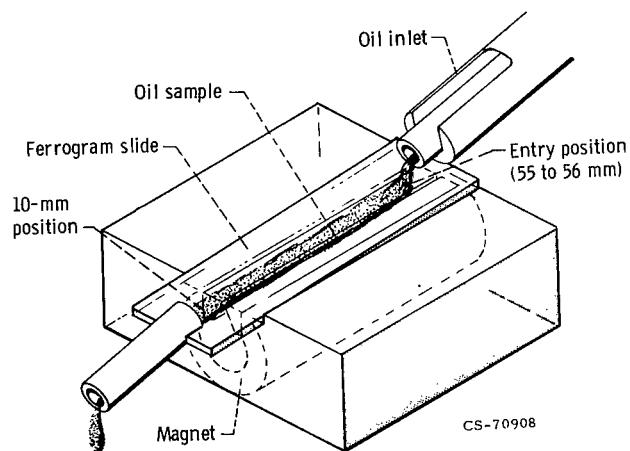
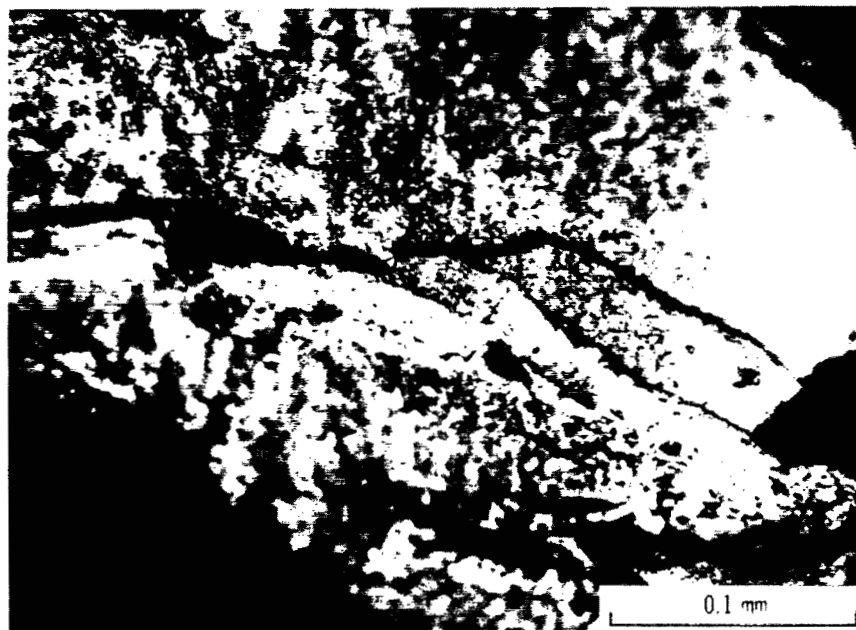


Figure 2. - Ferrograph analyzer.



(a) Typical spall.



(b) Enlarged portion of (a).

Figure 3. - Fatigue spall.

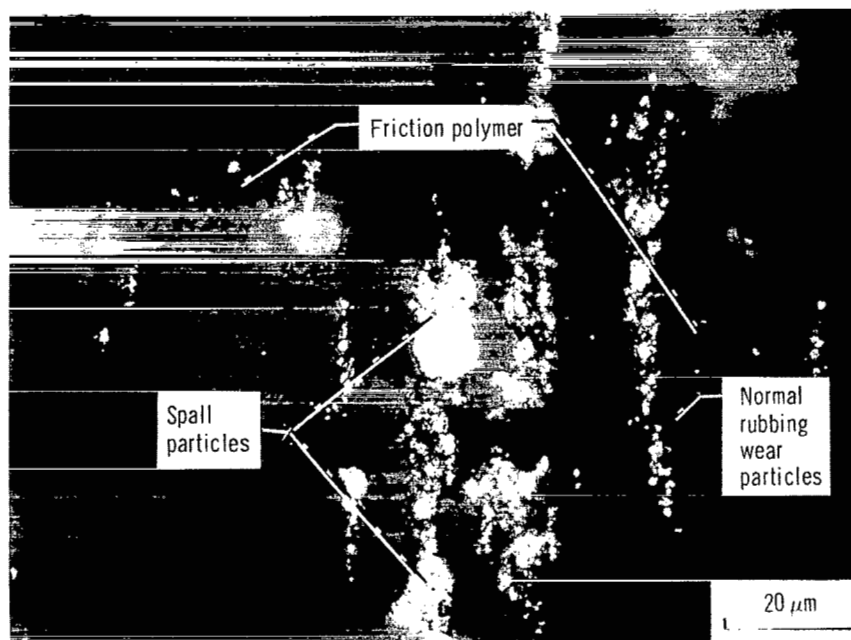
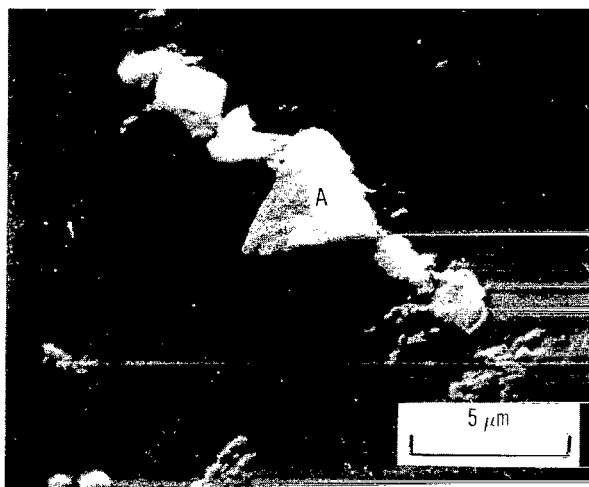
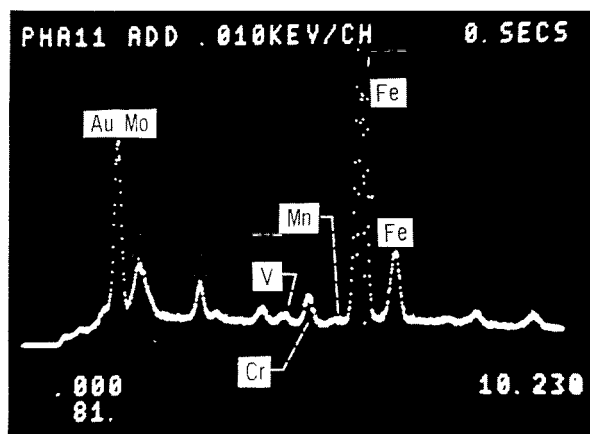


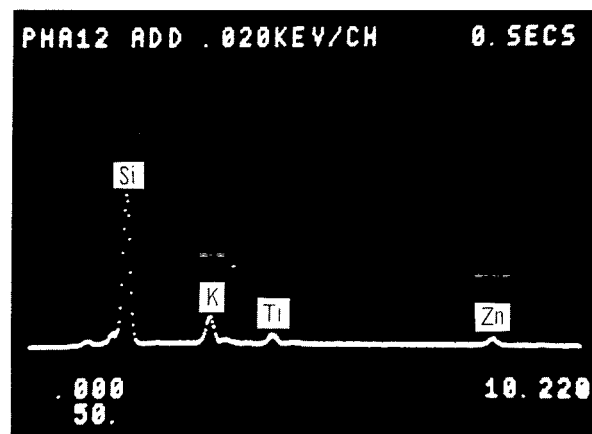
Figure 4. - Ferrogram entry deposit from test F-6 (76 hr).



(a) Electron micrograph of wear debris from test F-7 (98 hr).

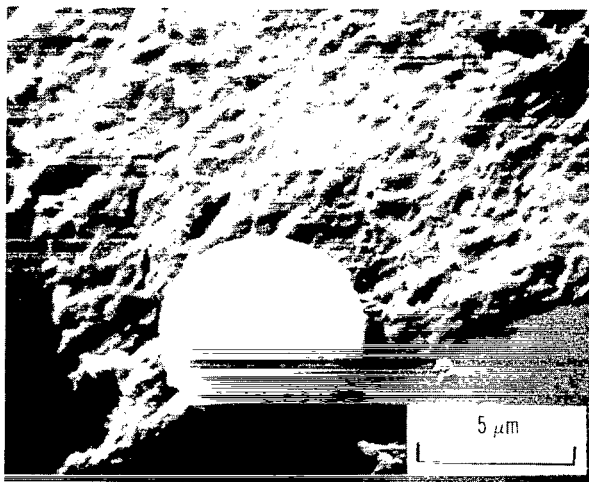


(b) Energy dispersive X-ray analysis (EDAX) of particle A.

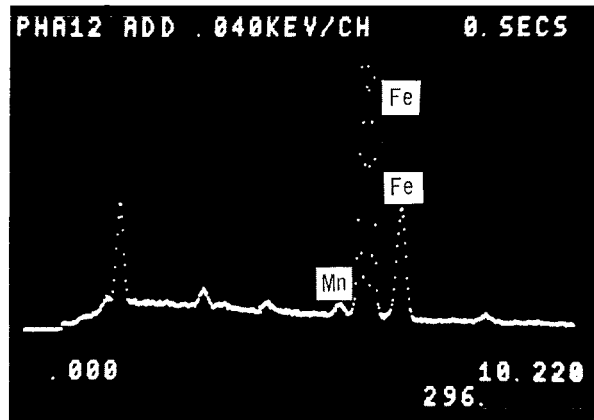


(c) Background EDAX of Ferrogram.

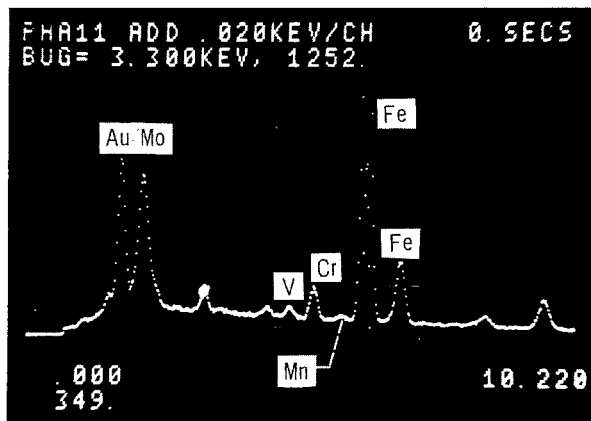
Figure 5. - Rubbing wear particles.



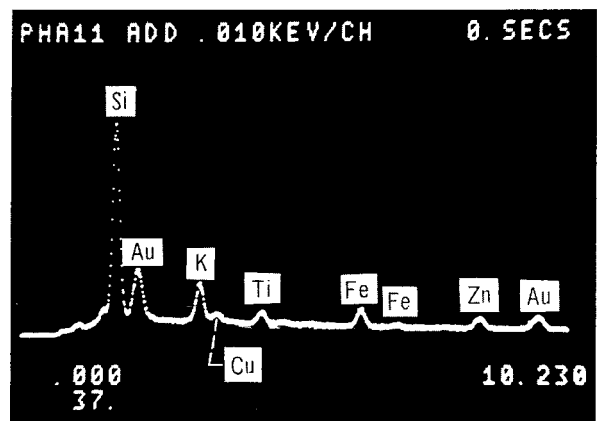
(a) Electron micrograph of spherical particle and friction polymer from test F-7 (98 hr).



(b) EDAX of spherical particles.

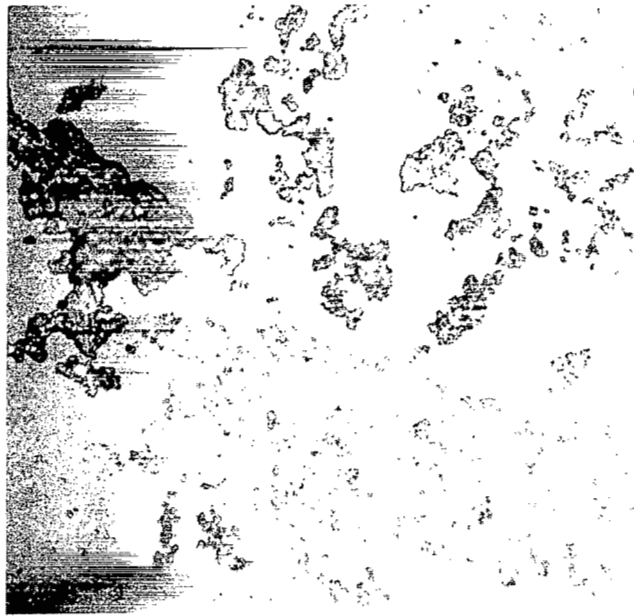


(c) EDAX of spherical particles.

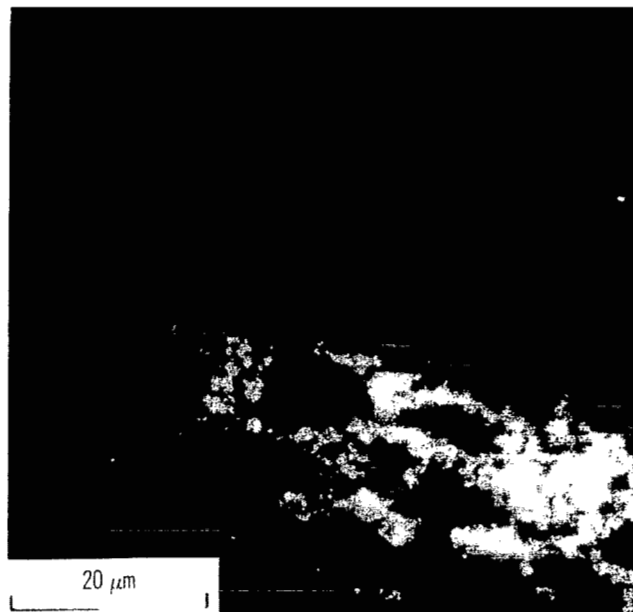


(d) EDAX of friction polymer.

Figure 6. - Friction polymer and spherical particle.



(a) Reflected light.



(b) Reflected polarized light with crossed analyzer.

Figure 7. - Friction polymer deposit from test S-4 (27 hr).

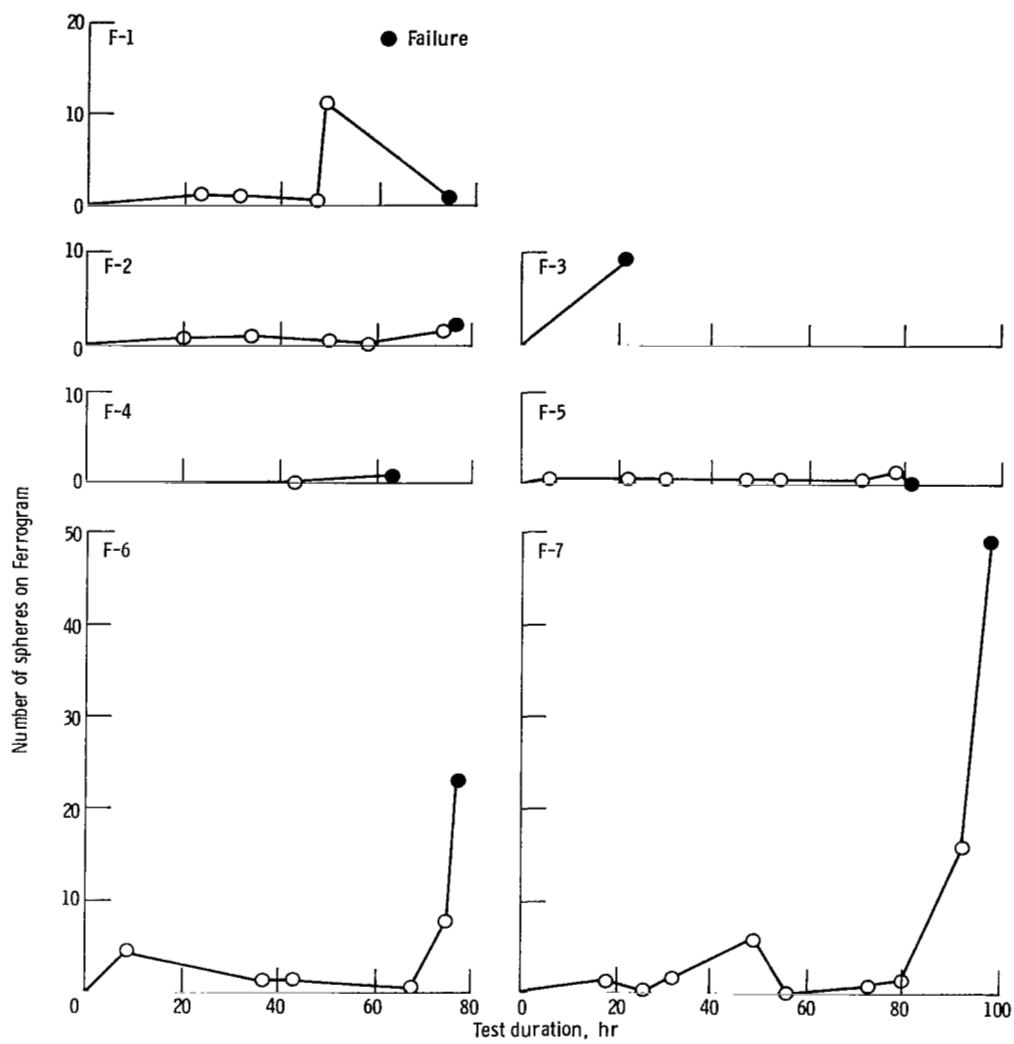


Figure 8. - Number of spheres on Ferrogram as function of test duration - failures.

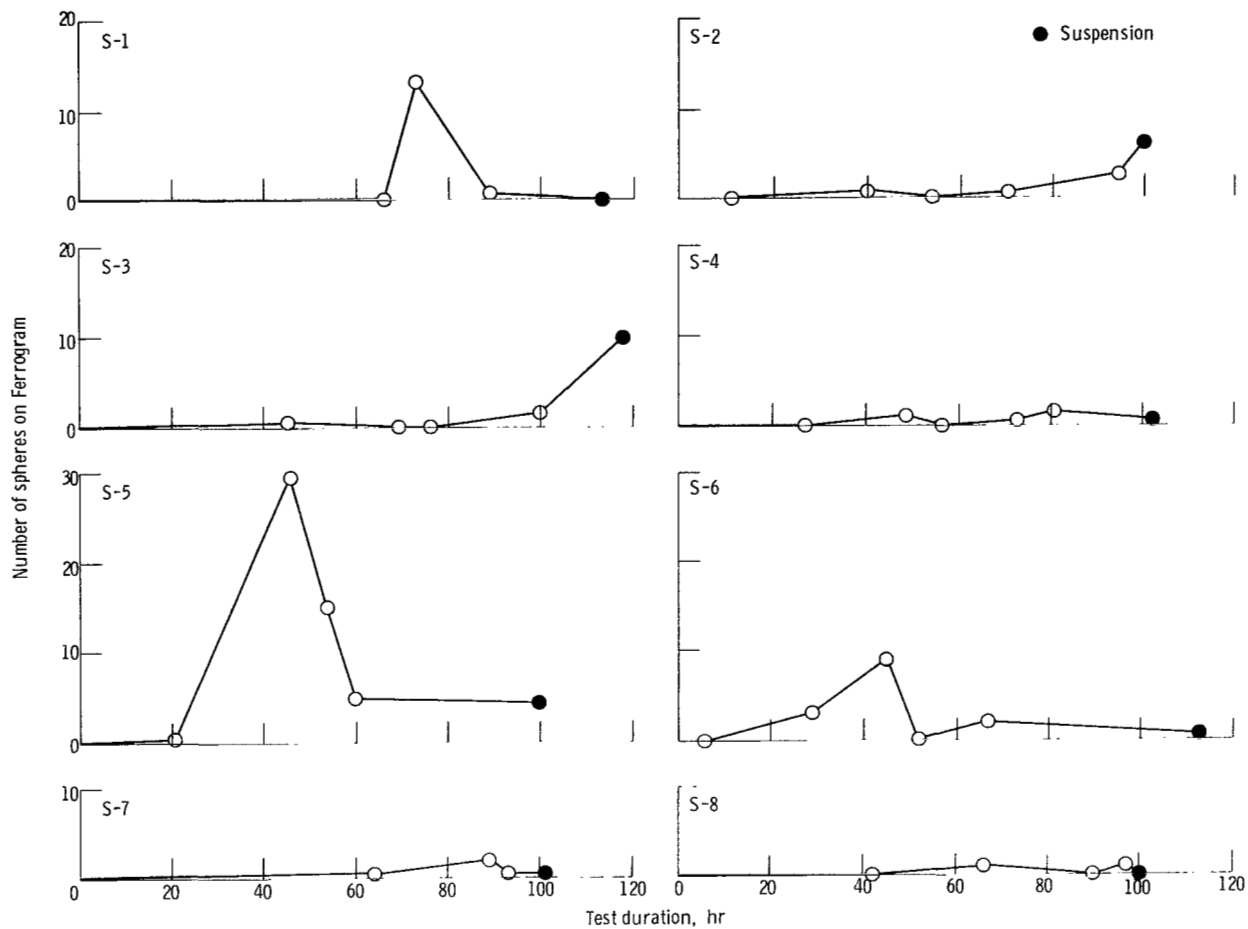


Figure 9. - Number of spheres on Ferrogram as functions of test duration - suspensions.

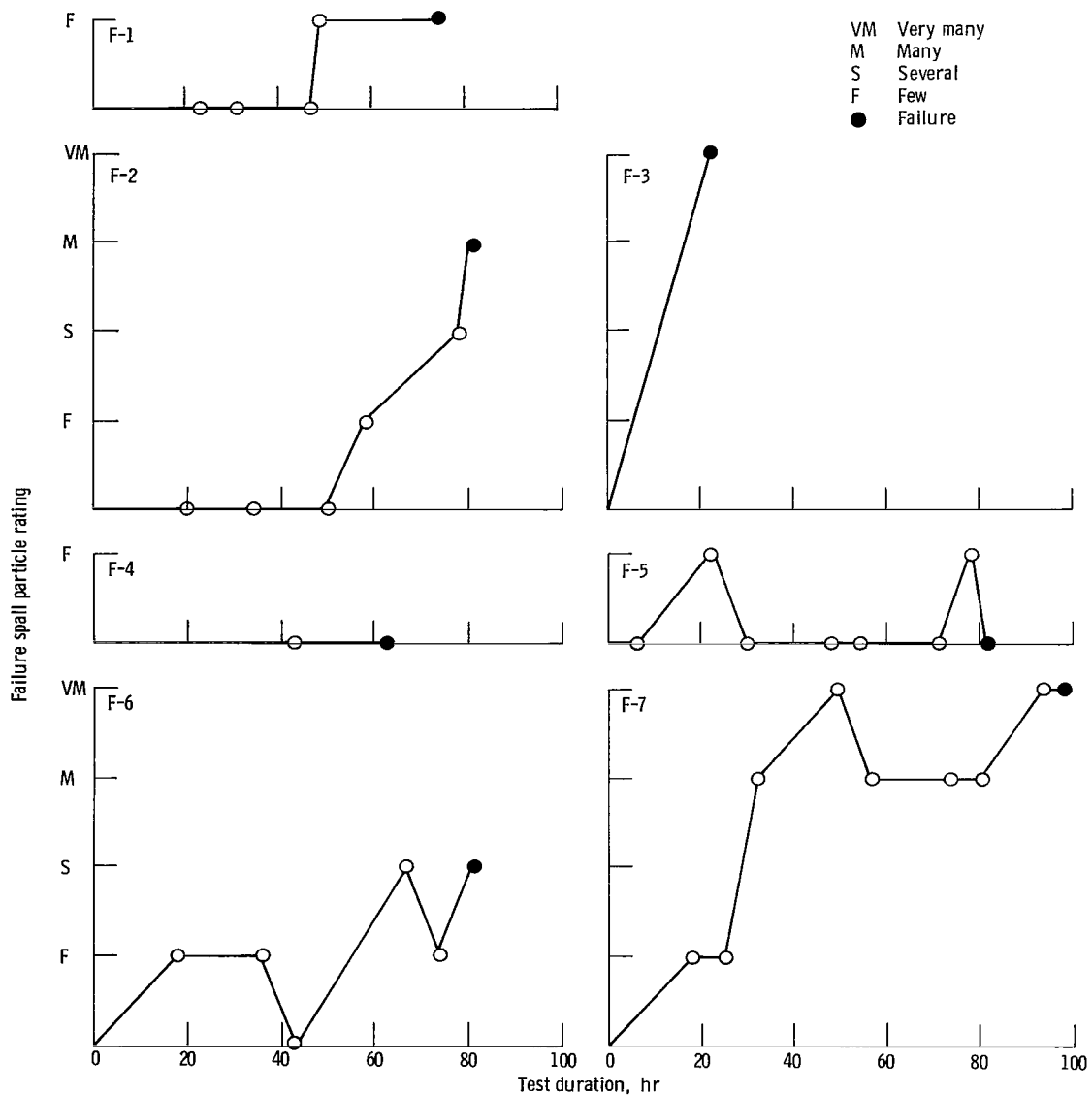


Figure 10. - Fatigue spall particle rating as function of test duration - failures.

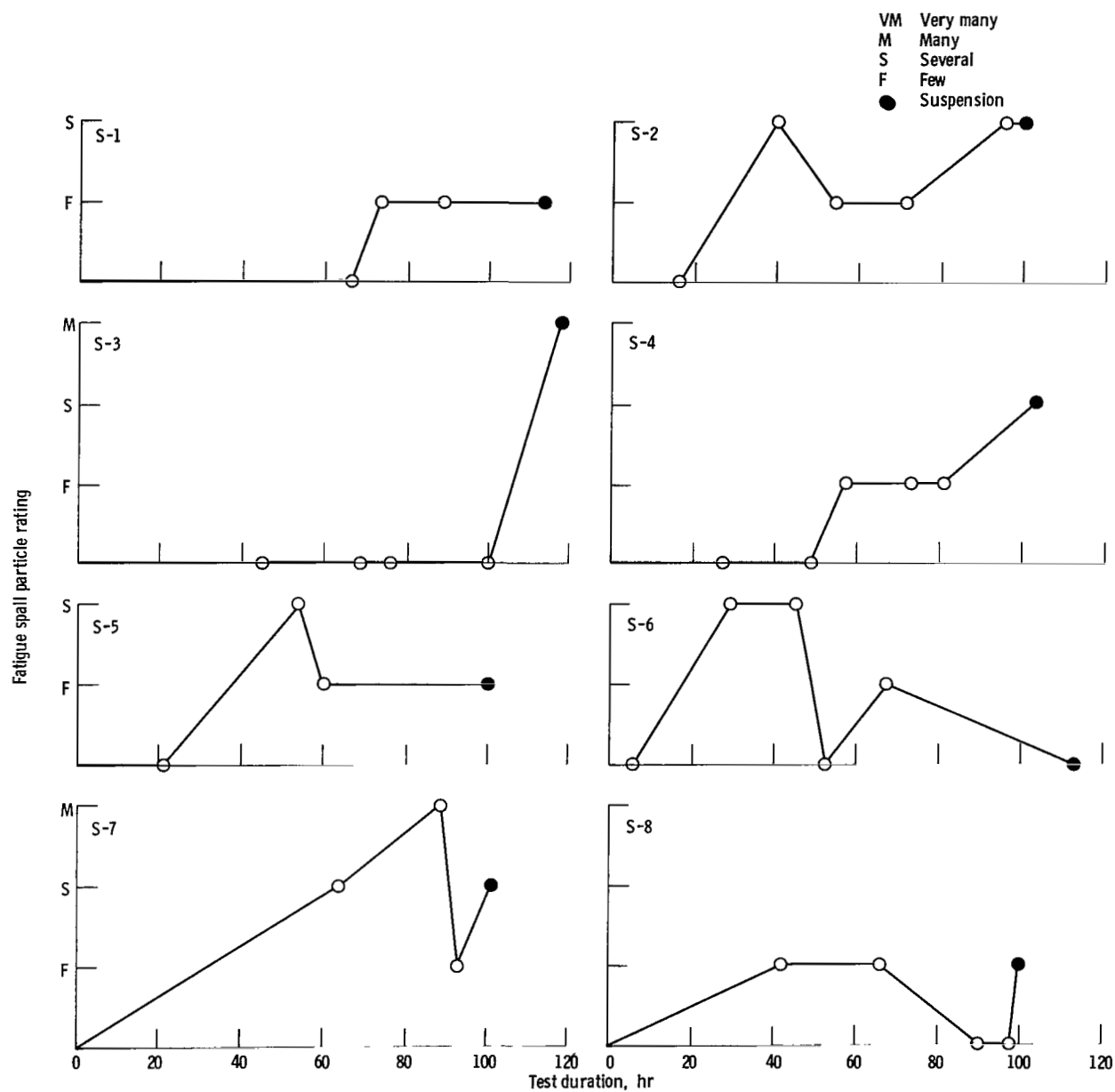


Figure 11. - Fatigue spall particle rating as function of test duration - suspensions.

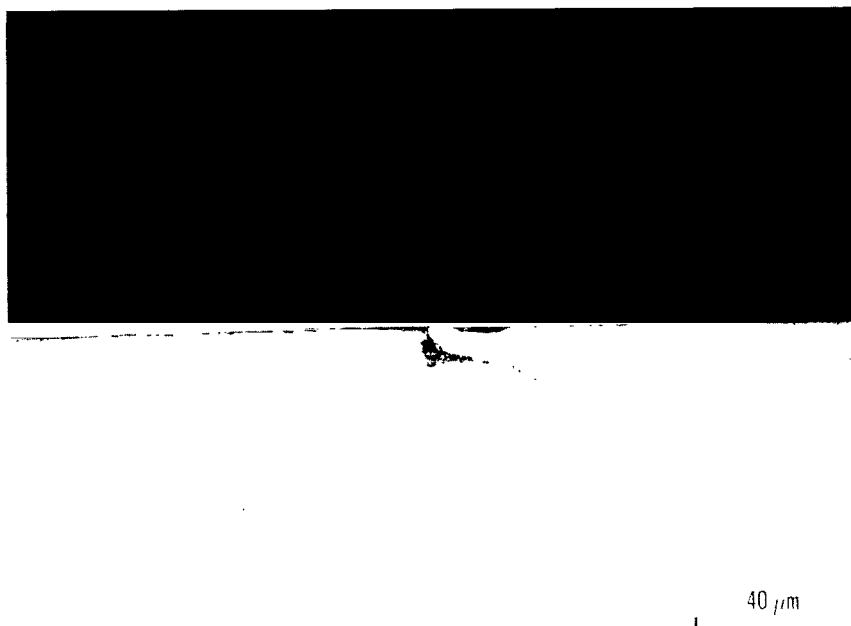


Figure 12. - Optical micrograph of sectioned wear track showing a surface crack (upper test ball, S-8, 100 hr).

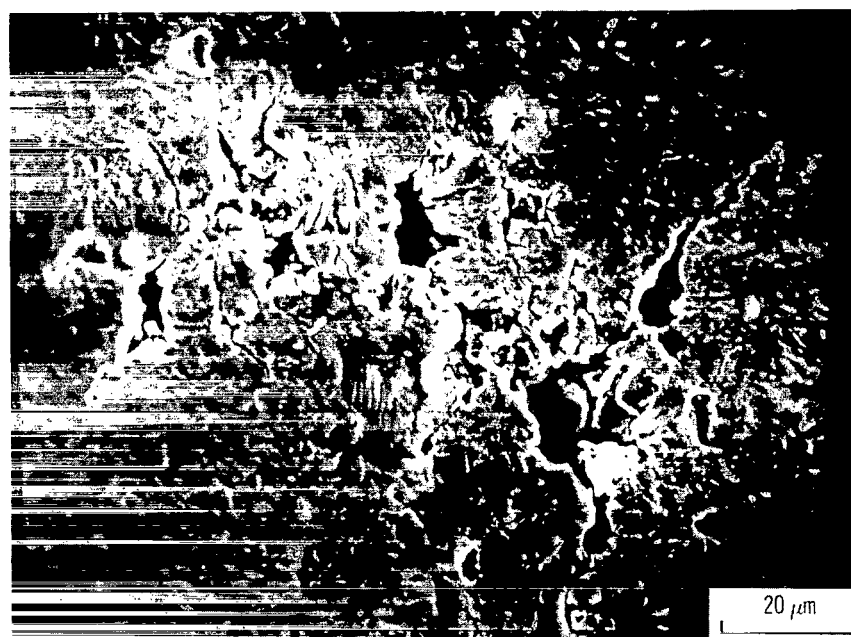


Figure 13. - Electron micrograph of wear track showing surface damage (upper test ball, S-5, 100 hr).

1. Report No. NASA TP-1203	2. Government Accession No.	3. Recipient's Catalog No.
4. Title and Subtitle CHARACTERIZATION OF WEAR DEBRIS GENERATED IN ACCELERATED ROLLING-ELEMENT FATIGUE TESTS	5. Report Date April 1978	6. Performing Organization Code
7. Author(s) William R. Jones, Jr., and Richard J. Parker	8. Performing Organization Report No. E-9260	10. Work Unit No. 505-04
9. Performing Organization Name and Address National Aeronautics and Space Administration Lewis Research Center Cleveland, Ohio 44135	11. Contract or Grant No.	13. Type of Report and Period Covered Technical Paper
12. Sponsoring Agency Name and Address National Aeronautics and Space Administration Washington, D.C. 20546	14. Sponsoring Agency Code	
15. Supplementary Notes		
16. Abstract <p>A Ferrographic analysis was used to determine the types and quantities of wear debris generated during accelerated rolling contact fatigue tests. The NASA five-ball rolling contact fatigue tester was used. Ball specimens were made of AMS 5749, a corrosion resistant, high-temperature bearing steel. The lubricant was a superrefined naphthenic mineral oil. Conditions included a maximum Hertz stress of 5.52×10^9 Pa and a shaft speed of 10 000 rpm. Four types of wear debris were observed - normal rubbing wear particles, fatigue microspall particles, spheres, and friction polymer deposits. The characterization of wear debris as a function of time was of limited use in predicting fatigue failures in these accelerated tests.</p>		
17. Key Words (Suggested by Author(s)) Ferrographic analysis Rolling-element fatigue Bearings	18. Distribution Statement Unclassified - unlimited STAR Category 37	
19. Security Classif. (of this report) Unclassified	20. Security Classif. (of this page) Unclassified	21. No. of Pages 26
		22. Price* A03

* For sale by the National Technical Information Service, Springfield, Virginia 22161



National Aeronautics and
Space Administration

Washington, D.C.
20546

Official Business

Penalty for Private Use, \$300

THIRD-CLASS BULK RATE

Postage and Fees Paid
National Aeronautics and
Space Administration
NASA-451



19 1 10, D, 040878 S00903DS
DEPT OF THE AIR FORCE
AF WEAPONS LABORATORY
ATTN: TECHNICAL LIBRARY (SUL)
KIRTLAND AFB NM 87117

NASA

POSTMASTER:

If Undeliverable (Section 158
Postal Manual) Do Not Return